A Triiron Complex Containing the Carboxylate-Free $\{Fe_3(\mu_3\text{-}O)\}^{7+}$ Core and Distorted Pentagonal-Bipyramidal Metal Centres

Subramanya Gupta Sreerama[a] and Samudranil Pal*[a]

Keywords: Trinuclear iron(III) complex / Crystal structure / Magnetic properties / Redox properties

The reaction of $Fe(ClO_4)_3\cdot 6H_2O$, 1,2-bis(biacetylmonoximeimino)ethane (H_2bamen) and triethylamine (1:1:2 mol ratio) in methanol affords a trinuclear complex with the formula $[Fe_3(\mu_3\text{-}O)(\mu_3\text{-bamen})_3]ClO_4\cdot 2H_2O$. The structure of the complex cation in this species shows a symmetric planar central $\{Fe_3(\mu_3\text{-}O)\}^{7+}$ unit coordinated to three N_4O_2 donor bridging (via oximate groups) ligands ($bamen^{2-}$). The N_4O_3 coordination sphere around each metal centre is very close to pentagonal-bipyramidal. Four N atoms of one $bamen^{2-}$ and the oxo group satisfy five coordination sites and form a pentagonal plane around the metal ion. The axial sites are occupied by two oximato O atoms from the other two $bamen^{2-}$ ligands. Thus, in addition to the μ_3-oxo group, two oximate groups provide two additional bridges between each pair of metal centres. In the crystal lattice, the water molecules exist as hydrogen-bonded dimers and these water dimers together with the perchlorate ions form a hydrogen-bond-supported helix. The complex cations form a chain via C–H···O interactions involving a methyl group and a metal-coordinated oximato O atom. The helix of $\{(H_2O)_2ClO_4^-\}$ units and the chain of $[Fe_3O(bamen)_3]^+$ cations are connected by O–H···O interactions which involve a water molecule and a second oximato O atom. In its cyclic voltammogram, the complex displays metal-centred oxidation as well as reduction responses. Variable-temperature magnetic susceptibility measurements revealed the presence of an antiferromagnetic interaction [J = –41.0(2) cm^{-1}] between the Fe^{III} centres in this complex.

Introduction

Trinuclear μ_3-oxo-bridged transition metal ion complexes have been of considerable interest for their molecular structures, magnetic properties and intramolecular electron transfer features in the mixed-valence variety. Such complexes are also useful precursors for the synthesis of higher nuclearity metal clusters. A number of complexes containing the $\{M_3(\mu_3\text{-}O)\}$ unit have been reported.[1–11] Essentially in all of them, the triangular metal ion core with the central oxo bridge is stabilised by six carboxylate groups (RCO_2^-) and three monodentate ligands (L). In these complexes of general formula $[M_3(\mu_3\text{-}O)(\mu_2\text{-}O_2CR)_6L_3]^{0/+}$, each metal ion is in a distorted octahedral coordination sphere. The O atoms of the bridging carboxylate groups constitute an O_4 square plane and the μ_3-O and the monodentate ligand L occupy the remaining two *trans* sites. The central $\{M_3(\mu_3\text{-}O)\}$ core is usually planar and has close to threefold symmetry. Complexes of $\{M_3(\mu_3\text{-}O)\}$ without carboxylate ligands are very rare although a few mixed-ligand complexes of this type are known.[12,13] However, in these complexes the $\{M_3(\mu_3\text{-}O)\}$ unit is asymmetric and pyramidal. Recently, we reported a carboxylate-free trinuclear complex containing the planar and symmetric $\{Mn_3(\mu_3\text{-}O)\}^{7+}$ core with a Schiff base (H_2bamen, two H represent the dissociable oxime protons) derived from 1 equiv. of ethylenediamine and 2 equiv. of biacetylmonoxime.[14] The metal ions in $[Mn_3(\mu_3\text{-}O)(\mu_3\text{-bamen})_3]^+$ are in a distorted pentagonal-bipyramidal N_4O_3 coordination sphere. A ferromagnetic interaction is operative between the metal ions in this complex. In contrast, the known μ_3-oxo-bridged trimanganese(III) complexes with carboxylate groups of formula $[Mn_3(\mu_3\text{-}O)(\mu_2\text{-}O_2CR)_6(py)_3]^+$ are antiferromagnetic.[3] Because of this variation, and also to examine whether the stabilisation of the $\{Mn_3(\mu_3\text{-}O)\}^{7+}$ unit by three $bamen^{2-}$ ligands is unique or can be extended to Fe^{III}, we attempted to synthesise the triiron(III) analogue of $[Mn_3(\mu_3\text{-}O)(\mu_3\text{-bamen})_3]^+$ and compare its structure and properties with the known $[Fe_3(\mu_3\text{-}O)(\mu_2\text{-}O_2CR)_6L_3]^+$ complexes. Indeed we were able to isolate the trinuclear μ_3-oxo-bridged Fe^{III} complex using H_2bamen. In the following account, we describe the synthesis, X-ray structure and physical properties of $[Fe_3(\mu_3\text{-}O)(\mu_3\text{-bamen})_3]ClO_4\cdot 2H_2O$.

Results and Discussion

Synthesis and Characterisation of $[Fe_3O(bamen)_3]ClO_4\cdot 2H_2O$

The complex was synthesised in good yield by allowing $Fe(ClO_4)_3\cdot 6H_2O$, H_2bamen and triethylamine to react in a

[a] School of Chemistry, University of Hyderabad, Hyderabad 500046, India
Fax: (internat.) + 91-40-2301-2460
E-mail: spsc@uohyd.ernet.in

  DOI: 10.1002/ejic.200400427

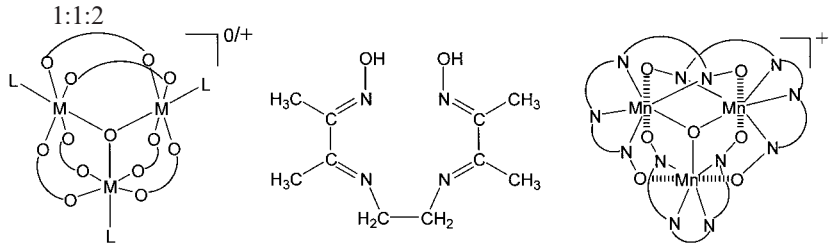

molar ratio in methanol under aerobic conditions. It precipitates as a brown solid from the reaction mixture. The elemental analysis data are satisfactory for the assigned molecular formula. In CH_3CN solution, the molar conductivity value of the complex (152 Ω^{-1} cm^2 M^{-1}) is consistent with 1:1 electrolytic behaviour.[15]

The infrared spectrum of the complex does not display any peak near 3000 cm^{-1}. The oxime OH groups of the ligands are therefore deprotonated. A broad peak centred at 3500 cm^{-1} is most likely due to the lattice water molecules. The presence of perchlorate is indicated by the bands at 1090 and 621 cm^{-1}. Two strong bands can be observed at 1641 and 1533 cm^{-1}. Comparable bands observed for complexes with dioxime ligands have been attributed to the coupled C···N and C···C stretching modes.[16] There is a 1:1 correlation between the infrared spectrum of this complex and that of $[Mn_3O(bamen)_3]ClO_4{\cdot}2H_2O$.[14] This observation, together with the elemental analysis and molar conductivity data, suggests that the present complex is most likely the Fe^{III} analogue of $[Mn_3O(bamen)_3]ClO_4{\cdot}2H_2O$.

The electronic spectrum of the complex in CH_3CN solution shows a weak absorption at 720 nm followed by three strong absorptions in the range of 383−248 nm. Weak absorptions observed for $[Fe_3O(O_2CR)_6(H_2O)_3]^+$ in the range of 980−625 nm have been assigned to d-d transitions and the large extinction coefficients which are unusual for spin-forbidden transitions can be attributed to the spin-exchange between the metal ions.[1] The higher energy intense absorptions are most likely due to ligand-to-metal and intraligand charge transfer transitions.[16]

Structure of $[Fe_3O(bamen)_3]^+$

An X-ray crystallographic study revealed that $[Fe_3O(bamen)_3]ClO_4{\cdot}2H_2O$ is isomorphous with the corresponding Mn^{III} analogue $[Mn_3O(bamen)_3]ClO_4{\cdot}2H_2O$.[13] Both species crystallise in the same space group with very similar unit cell dimensions. The structure of $[Fe_3O(bamen)_3]^+$ is illustrated in Figure 1. The cation contains three bridging N_4O_2 donor bamen^{2-} ligands, one μ_3-oxo group and three metal centres. The presence of one ClO_4^- anion per complex cation indicates that the oxidation state of each metal centre is +3. The C−N and N−O bond lengths in the oximate [−(CH$_3$)C=N−O$^-$] fragments are in the ranges 1.277(4)−1.288(4) Å and 1.337(4)−1.353(4) Å, respectively. These bond lengths are similar to the corresponding ones reported for deprotonated oxime functionalities.[14,17] All other intraligand bond parameters are unexceptional. The metal ions are heptacoordinated and each bamen^{2-} is coordinated to all three Fe atoms. Four N atoms coordinate one metal centre forming three five-membered chelate rings and the two oximato O atoms coordinate to the other two metal centres. As a result, each pair of iron centres is bridged by two oximate groups (=N−O$^-$) in a reciprocal fashion with respect to the N and O atom coordination. The seventh coordination site is satisfied by the μ_3-oxo atom. Thus, each metal ion has an N_4O_3 coordination sphere. The Fe−N_{imine} bond lengths [2.233(3)−2.250(3) Å] are significantly shorter than the Fe−$N_{oximate}$ bond lengths [2.302(3)−2.340(3) Å] (Table 1). This difference is possibly due to the bridging nature of the oximate groups and the rigidity of the N_4 fragment of the ligands.[14,18] The central $\{Fe_3(\mu_3\text{-}O)\}^{7+}$ core is essentially planar. The solid angle at the μ_3-O centre is 359.95° and its displacement from the Fe_3 plane is 0.024(2) Å. The Fe−μ_3-O bond lengths [1.898(2)−1.911(2) Å] and the Fe···Fe distances [3.2992(9)−3.3013(7) Å] are similar to the corresponding values reported for complexes containing the $\{Fe_3(\mu_3\text{-}O)\}^{7+}$ core.[6,9,11] The N_4O_3 coordination geometry around each Fe atom can be best described as pentagonal-bipyramidal. The four N atoms and the μ_3-O atom constitute the pentagonal plane and the two oximato O

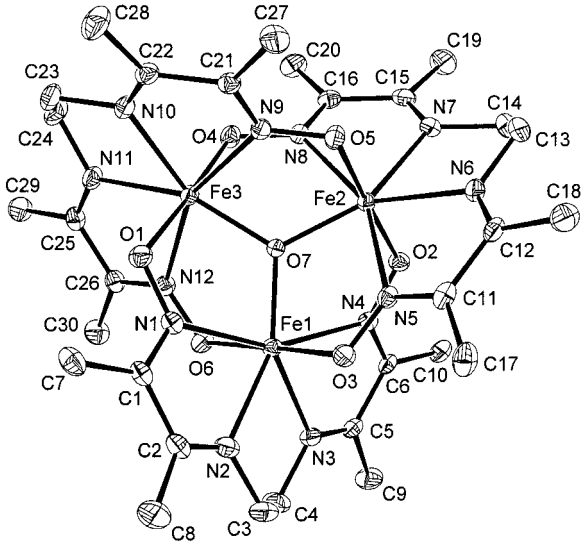

Figure 1. Structure of $[Fe_3(\mu_3\text{-}O)(\mu_3\text{-bamen})_3]^{3+}$ with the atom-labelling scheme; all atoms are represented by their 25% probability thermal ellipsoids; hydrogen atoms are omitted for clarity

Table 1. Selected bond lengths [Å] and bond angles [°] for $[Fe_3O(bamen)_3]ClO_4{\cdot}2H_2O$

Fe(1)−N(1)	2.326(3)	Fe(2)−O(2)	1.987(2)
Fe(1)−N(2)	2.247(3)	Fe(2)−O(5)	1.983(2)
Fe(1)−N(3)	2.236(3)	Fe(2)−O(7)	1.908(2)
Fe(1)−N(4)	2.341(3)	Fe(3)−N(9)	2.334(3)
Fe(1)−O(3)	1.979(2)	Fe(3)−N(10)	2.251(3)
Fe(1)−O(6)	1.982(2)	Fe(3)−N(11)	2.236(3)
Fe(1)−O(7)	1.910(2)	Fe(3)−N(12)	2.311(3)
Fe(2)−N(5)	2.302(3)	Fe(3)−O(1)	1.997(2)
Fe(2)−N(6)	2.235(3)	Fe(3)−O(4)	1.989(2)
Fe(2)−N(7)	2.233(3)	Fe(3)−O(7)	1.898(2)
Fe(2)−N(8)	2.334(3)		
N(1)−Fe(1)−N(2)	67.57(11)	O(2)−Fe(2)−N(8)	94.72(10)
N(2)−Fe(1)−N(3)	72.31(12)	O(2)−Fe(2)−O(7)	90.85(10)
N(3)−Fe(1)−N(4)	67.28(11)	O(5)−Fe(2)−N(5)	91.75(10)
N(4)−Fe(1)−O(7)	77.48(10)	O(5)−Fe(2)−N(6)	80.73(10)
O(7)−Fe(1)−N(1)	78.43(10)	O(5)−Fe(2)−N(7)	98.73(11)
O(3)−Fe(1)−N(1)	93.53(10)	O(5)−Fe(2)−N(8)	87.04(10)
O(3)−Fe(1)−N(2)	81.43(11)	O(5)−Fe(2)−O(7)	90.92(10)
O(3)−Fe(1)−N(3)	96.64(11)	N(9)−Fe(3)−N(10)	67.00(10)
O(3)−Fe(1)−N(4)	86.04(10)	N(10)−Fe(3)−N(11)	72.47(11)
O(3)−Fe(1)−O(7)	90.74(10)	N(11)−Fe(3)−N(12)	68.15(11)
O(6)−Fe(1)−N(1)	84.22(10)	N(12)−Fe(3)−O(7)	78.17(10)
O(6)−Fe(1)−N(2)	96.12(11)	O(7)−Fe(3)−N(9)	77.28(10)
O(6)−Fe(1)−N(3)	83.88(10)	O(1)−Fe(3)−N(9)	94.17(10)
O(6)−Fe(1)−N(4)	96.71(10)	O(1)−Fe(3)−N(10)	82.03(11)
O(6)−Fe(1)−O(7)	90.48(10)	O(1)−Fe(3)−N(11)	95.20(11)
N(5)−Fe(2)−N(6)	68.24(11)	O(1)−Fe(3)−N(12)	83.45(10)
N(6)−Fe(2)−N(7)	72.52(12)	O(1)−Fe(3)−O(7)	92.02(10)
N(7)−Fe(2)−N(8)	67.48(11)	O(4)−Fe(3)−N(9)	87.01(10)
N(8)−Fe(2)−O(7)	77.21(10)	O(4)−Fe(3)−N(10)	96.08(11)
O(7)−Fe(2)−N(5)	77.99(10)	O(4)−Fe(3)−N(11)	82.20(11)
O(2)−Fe(2)−N(5)	87.24(10)	O(4)−Fe(3)−N(12)	96.56(11)
O(2)−Fe(2)−N(6)	97.02(11)	O(4)−Fe(3)−O(7)	90.75(10)
O(2)−Fe(2)−N(7)	80.69(10)		

atoms occupy the two axial sites. The mean deviations from the pentagonal $N_4(\mu_3\text{-}O)$ plane are in the range 0.21−0.22 Å. The $O_{oximate}$−Fe−N/O7 angles fall in the range 80.69(10)−98.73(11)° and the $O_{oximate}$−Fe−$O_{oximate}$ angles are within 177.17(10)−177.74(10)°.

Hydrogen Bonding and Crystal Packing

In the crystal lattice of $[Fe_3O(bamen)_3]ClO_4{\cdot}2H_2O$, the water molecules and the perchlorate ions exist in a helical fashion through hydrogen bonding interactions (Figure 2). Two water molecules form a linear dimer [O···O distance, 2.890(8) Å; O−H···O angle, 149.8°]. The hydrogen bond acceptor molecule in this water dimer is again hydrogen-bonded to one perchlorate oxygen atom [O···O distance, 3.119(8) Å; O−H···O angle, 142.8°]. The donor water molecule of the dimer in the $\{(H_2O)_2ClO_4^-\}$ unit is hydrogen-bonded with a perchlorate oxygen atom (O···O distance, 3.026(8) Å; O−H···O angle, 160.3°) of a symmetry-related $\{(H_2O)_2ClO_4^-\}$ unit. These three hydrogen bonding interactions lead to the helical arrangement of the water molecules and the perchlorate ions (Figure 2). Interestingly, the cations also exist in a chain-like arrangement via inter-cation C−H···O interactions [C···O distance, 3.346(5) Å; C−H···O angle, 147.4°] involving a methyl group (C17) and an oximato O atom (O6).[19−21] Another metal-coordinated oximato O atom (O1) and the O atom of the acceptor molecule in the water dimer present in the $\{(H_2O)_2ClO_4^-\}$ unit are within hydrogen bond lengths [O···O distance, 3.201(7) Å; O−H···O angle, 128.1°]. This is also reflected in the rather long Fe3−O1 bond [1.997(2) Å] compared with the other Fe−$O_{oximate}$ bonds [1.979(2)−1.989(2) Å]. Thus, the chain of cations and the helix of $\{(H_2O)_2ClO_4^-\}$ units are bridged by O−H···O interactions (Figure 3). There are no other inter-chain or inter-helix noncovalent interactions. The same packing arrangement of the water molecules, the perchlorates and the complex cations can be observed in the crystal lattice of $[Mn_3O(bamen)_3]ClO_4{\cdot}2H_2O$.[14]

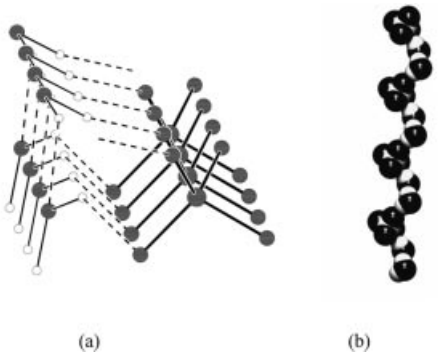

Figure 2 Helical arrangement of the $\{(H_2O)_2ClO_4^-\}$ units: (a) propagation of the helix through the hydrogen bonding interactions; (b) space-filling model of the helix

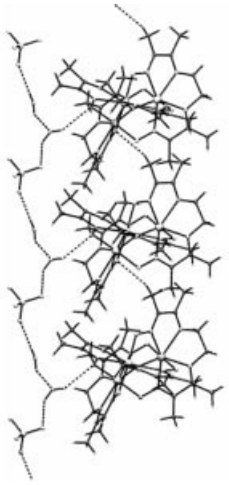

Figure 3. Ball-and-stick representation of the chain of complex cations and the helix of $\{(H_2O)_2ClO_4^-\}$ units connected by O−H···O interactions

Redox Properties

The electron transfer behaviour of $[Fe_3O(bamen)_3]ClO_4{\cdot}2H_2O$ in CH_3CN has been studied using cyclic voltammetry. The complex displays a reversible oxidation response at $E_{1/2}$ = 1.05 V (ΔE_p = 80 mV) and another reversible reduction response at $E_{1/2}$ = −1.05 V (ΔE_p = 60 mV) (Figure 4). The peak currents observed for these two responses are similar to the peak currents of known one-electron processes under identical conditions.[18,22] The depro-

tonated ligand ($bamen^{2-}$) does not display any response in the potential range +2.1 to −2.1 V. Thus, the oxidation response can be assigned to the $Fe^{III}{}_2Fe^{IV}/Fe^{III}{}_3$ couple and the reduction response to the $Fe^{III}{}_3/Fe^{III}{}_2Fe^{II}$ couple. On the anodic side of the SCE, in addition to the reversible oxidation response, two more irreversible oxidation responses (E_{pa} = 1.41 and 1.75 V) can be observed. However, the peak current of the lower potential response is 1/3rd and that of the higher potential response is almost double the peak current of the reversible oxidation response. The corresponding Mn^{III} analogue displays two reversible and one irreversible metal-centred oxidations.[14] Thus, the irreversible oxidations observed for the present complex may perhaps involve the metal centres. However, the irreversible nature clearly indicates that the corresponding oxidised species are unstable in the cyclic voltammetric time scale. Similarly, on the cathodic side of the SCE, an irreversible reduction at −1.66 V having a peak current similar to that of the reversible reduction response was observed. This response may be due to the $Fe^{III}{}_2Fe^{II} \rightarrow Fe^{III}Fe^{II}{}_2$ process as the ligand is redox inactive at this potential. It is interesting to note that there are no reports of metal-centred oxidations displayed by $[M_3O(O_2CR)_6L_3]^+$ species containing first row metal ions. Normally for these species, metal-centred reductions are observed and very few of them display more than one reversible redox step.[9]

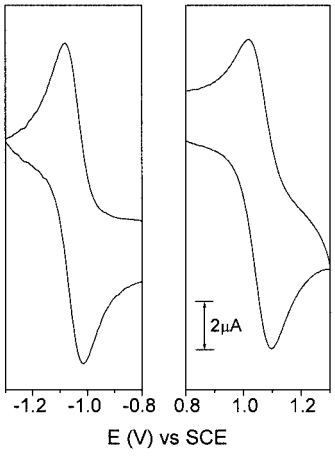

Figure 4. Cyclic voltammograms (scan rate 50 mV s^{-1}) of $[Fe_3O(bamen)_3]ClO_4{\cdot}2H_2O$ in acetonitrile (0.1 M TBAP) at a platinum electrode (298 K)

Magnetic Properties

A powdered sample of $[Fe_3O(bamen)_3]ClO_4{\cdot}2H_2O$ was used for the measurements of the magnetic susceptibilities at a fixed magnetic field of 5 kG in the temperature range 18−300 K. The effective magnetic moment of the complex at 300 K is 5.00 μ_B. The moment gradually decreases with the lowering of the temperature and reaches a value of 1.71 μ_B at 18 K. The nature of the curve obtained by plotting the moment against temperature (Figure 5) clearly indicates the antiferromagnetic character of the complex and the value of the moment at the lowest temperature is consistent with an S = 1/2 ground state. The data were fitted using an expression for χ_M vs. T obtained from the isotropic spin exchange Hamiltonian $H = -2J(S_1S_2 + S_2S_3 + S_3S_1)$ for a triangular triiron(III) complex in which all the metal ions are equivalent and have the same spin state $S_1 = S_2 = S_3 = 5/2$.[23] The best least-squares fit[24] was obtained with $J = -41.0(2)$ cm^{-1} and $g = 1.984(4)$ ($R = 1.50 \times 10^{-4}$). Complexes of formula $[Fe_3(\mu_3\text{-}O)(\mu_2\text{-}O_2CR)_6L_3]^+$ are known to be antiferromagnetic and the J values reported for such species span the range −15 to −33 cm^{-1}.[1,3−5,11] It has also been noted that the antiferromagnetic interaction decreases as the metal ion is changed from Fe^{III} to Mn^{III} in the acetate complexes of $\{M_3(\mu_3\text{-}O)\}^{7+}$. In this type of species, the metal ions are in a distorted octahedral coordination sphere. The unpaired electrons present in the σ-interacting e_g orbitals are involved in the antiferromagnetic exchange process. Thus, the decrease in the $-J$ value has been attributed to the decrease in the number of unpaired electrons in the e_g orbitals as one goes from high-spin Fe^{III} ($t_{2g}{}^3e_g{}^2$) to high-spin Mn^{III} ($t_{2g}{}^3e_g{}^1$).[3] Interestingly, the antiferromagnetic interaction in $[Fe_3O(bamen)_3]^+$ is noticeably higher than that in the $[Fe_3O(O_2CR)_6L_3]^+$ complexes and a ferromagnetic interaction [J = 22.3(1) cm^{-1}][14] is operative in $[Mn_3O(bamen)_3]^+$ rather than a weaker antiferromagnetic interaction as observed in $[Mn_3O(O_2CR)_6L_3]^+$. It is very likely that the change in the coordination geometry around the metal ions from octahedral in $[M_3O(O_2CR)_6L_3]^+$ to pentagonal-bipyramidal in $[M_3O(bamen)_3]^+$ is primarily responsible for the differences in the magnetic properties of these two types of complex containing the same $\{M_3(\mu_3\text{-}O)\}^{7+}$ core. It may be noted that in the pentagonal-bipyramidal coordination sphere the highest energy d_{z^2} orbital in the high-spin Fe^{III} species will have an unpaired electron but that in the high-spin Mn^{III} species will be empty. Thus, the alteration in the nature of the spin-coupling from ferromagnetic in $[Mn_3O(bamen)_3]^+$ to antiferromagnetic in $[Fe_3O(bamen)_3]^+$ is perhaps dictated by the absence or presence of an electron in the d_{z^2} orbital of the metal ion.

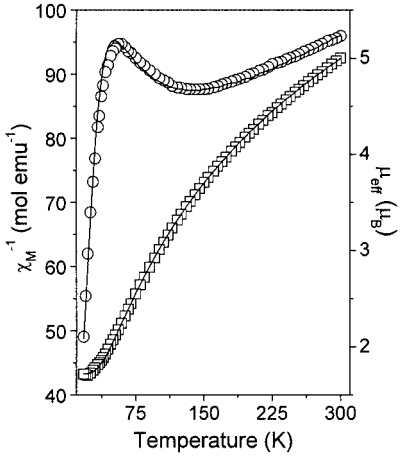

Figure 5. Temperature dependence of the inverse molar magnetic susceptibilities (open circles) and effective magnetic moments (open squares) of $[Fe_3O(bamen)_3]ClO_4{\cdot}2H_2O$; the continuous lines were generated from the best least-squares fit parameters given in the text

Conclusion

Before we reported the cationic complex $[Mn_3O(bamen)_3]^+$ [14], examples of carboxylate-free complexes containing the symmetric $\{M^{III}{}_3(\mu_3\text{-}O)\}$ unit were nonexistent. Now, we have been able to isolate the Fe^{III} analogue of the above complex. As in the Mn^{III} species, the metal ions in $[Fe_3O(bamen)_3]^+$ are in a pentagonal-bipyramidal N_4O_3 coordination sphere assembled by the bridging hexadentate N_4O_2 donor $bamen^{2-}$ and the μ_3-oxo group. Thus, like carboxylates, three $bamen^{2-}$ ligands are fairly efficient at stabilising the planar triangular ensemble of Mn^{III} and Fe^{III} ions with the central oxo bridge. A comparison of the redox and magnetic properties of $[M_3O(O_2CR)_6L_3]^+$ in which the metal ions are octahedral, with that of $[M_3O(bamen)_3]^+$ (M = Mn^{III} and Fe^{III}], reveals some interesting differences. Both $[M_3O(bamen)_3]^+$ species exhibit several metal-centred redox steps uncommon for $[M_3O(O_2CR)_6L_3]^+$ complexes. The $[M_3O(O_2CR)_6L_3]^+$ species are antiferromagnetic. However, the antiferromagnetic exchange is weaker in the Mn^{III} complexes than in the Fe^{III} complexes. On the other hand, $[Mn_3O(bamen)_3]^+$ is ferromagnetic whereas the Fe^{III} analogue is antiferromagnetic. The extent of antiferromagnetic coupling in $[Fe_3O(bamen)_3]^+$ is noticeably larger than in the carboxylate complexes of $\{Fe_3(\mu_3\text{-}O)\}^{7+}$.

Experimental Section

Materials: The Schiff base H_2bamen was prepared according to a reported procedure.[25] All other chemicals and solvents were of commercially available analytical grade and were used as received.

Physical Measurements: Microanalytical (C, H, N) data were obtained with a Perkin−Elmer Model 240C elemental analyser. A Shimadzu 3101-PC UV/Vis/NIR spectrophotometer was used to record the electronic spectrum. The infrared spectrum was collected in a KBr pellet with a Jasco-5300 FT-IR spectrophotometer. The variable-temperature (18−300 K) magnetic susceptibility measurements were performed using the Faraday technique with a set-up consisting of a George Associates Lewis coil force magnetometer, a CAHN microbalance and an Air Products closed-cycle helium cryostat. $Hg[Co(NCS)_4]$ was used as the standard. Diamagnetic corrections (-468×10^{-6} emu mol^{-1} for $[Fe_3O(bamen)_3]ClO_4{\cdot}2H_2O$) calculated from Pascal's constants[26] were used to obtain the molar paramagnetic susceptibilities. The solution electrical conductivity was measured with a Digisun DI-909 conductivity meter. A CH-Instruments model 620A electrochemical analyser was used for cyclic voltammetric experiments with an acetonitrile solution of the complex containing tetrabutylammonium perchlorate (TBAP) as the supporting electrolyte. The three electrode measurements were carried out at 298 K under nitrogen with a platinum working electrode, a platinum wire auxiliary electrode and a saturated calomel reference electrode (SCE). The potentials reported in this work are uncorrected for junction contributions.

Synthesis of $[Fe_3O(bamen)_3]ClO_4{\cdot}2H_2O$: A methanol solution (20 mL) of $Fe(ClO_4)_3{\cdot}6H_2O$ (1.022 g, 2.21 mmol) was added to a suspension of H_2bamen (500 mg, 2.21 mmol) in methanol (20 mL). The colour of the reaction mixture immediately became brown. To this brown solution was added triethylamine (435 mg, 4.3 mmol, 0.6 mL) and the reaction mixture was stirred in air at room temperature (298 K) for 8 h. The brown solid which precipitated was collected by filtration, washed with ice-cold methanol and finally dried in air. Recrystallisation was performed by dissolving the complex in a methanol/xylene mixture (2:1). Yield, 460 mg (63%). $C_{30}H_{52}ClFe_3N_{12}O_{13}$ (991.84): calcd. C 36.33, H 5.28; N 16.95; found C 36.12, H 5.48, N 17.13. Selected IR bands [cm^{-1}]: $\tilde{\nu}$ = 3500 br, 1641 s, 1533 s, 1431 m, 1379 m, 1323 m, 1188 m, 1090 vs, 692 s, 621 m, 592 m, 505 s, 411 s. Electronic spectroscopic data in CH_3CN: $\lambda_{max.}$ [nm] (ε [$M^{-1}\,cm^{-1}$]) = 720 (115), 383 (11 900), 277sh (37 900), 248 (47 800). Molar conductivity (CH_3CN): Λ_M [$\Omega^{-1}\,cm^2\,M^{-1}$] = 152.

X-ray Crystallography: Single crystals were grown by slow concentration of a methanol/xylene (2:1) solution of the complex. A crystal of dimensions 0.48 × 0.40 × 0.24 mm was used for data collection with an Enraf−Nonius Mach-3 diffractometer using graphite-monochromated Mo-K_α radiation (λ = 0.71073 Å) by the ω-scan method at 298 K. Unit cell parameters were determined by a least-squares fit of 25 reflections having θ values in the range 9−11°. Intensities of three check reflections were measured every 1.5 h during the data collection to monitor the crystal stability and no decay was observed. The ψ-scans[27] of 6 reflections having θ and χ values within 1−21° and 80−86°, respectively, were used for an empirical absorption correction. The structure was solved by direct methods in the $P\bar{1}$ space group and refined on F^2 by full-matrix least-squares procedures. The asymmetric unit contains a molecule of $[Fe_3O(bamen)_3]ClO_4$ and two water molecules. All non-H atoms were refined using anisotropic thermal parameters. The H atoms of the water molecules were located in a difference map and refined with geometric restraints with $U_{iso}(H) = 1.5U_{eq}(O)$. The remainder of the H atoms were included in the structure factor calculation in idealised positions using the riding model but they were not refined. The programs of the WinGX package[28] were used for data reduction and the absorption correction. The structure solution and refinement were performed with the SHELX-97 programs.[29] The ORTEX6a[30] and the PLATON[31] packages were used for molecular graphics. Selected crystal and refinement data are summarised in Table 2. Crystallographic data have been deposited with the

Table 2. Crystallographic data for $[Fe_3O(bamen)_3]ClO_4{\cdot}2H_2O$

Empirical formula	$C_{30}H_{52}ClFe_3N_{12}O_{13}$
Formula mass	991.84
Crystal system	triclinic
Space group	$P\bar{1}$
a [Å]	8.6821(9)
b [Å]	14.7950(11)
c [Å]	16.586(2)
α [°]	84.404(13)
β [°]	82.13(2)
γ [°]	85.970(8)
V [Å^3]	2096.9(4)
Z	2
μ [mm^{-1}]	1.162
Reflections collected	7389
Reflections unique	7389
Reflections [$I \geq 2\sigma(I)$]	5346
Parameters	544
$R1$, $wR2$ [$I \geq 2\sigma(I)$]	0.0381, 0.0889
$R1$, $wR2$ (all data)	0.0670, 0.1005
Goodness-of-fit on F^2	1.014
Largest peak, hole [eÅ^{-3}]	0.479, −0.449

Cambridge Crystallographic Data Centre (deposition number CCDC-239485). These data can be obtained from the CCDC, 12 Union Road, Cambridge, CB2 1EZ, UK; Fax: + 44-1233-336-033; E-mail: deposit@ccdc.cam.ac.uk.

Acknowledgments

Financial support for this work was provided by the Council of Scientific and Industrial Research (CSIR), New Delhi [Grant No. 01(1880)/03/EMR-II]. X-ray crystallographic data were obtained from the National Single Crystal Diffractometer Facility (established by the Department of Science and Technology, New Delhi) at the School of Chemistry, University of Hyderabad. Our sincere thanks are due to Prof. A. R. Chakravarty for providing the cryomagnetic data. We thank the University Grants Commission, New Delhi for the facilities provided under the Universities with Potential for Excellence program. S. G. S. thanks the CSIR for a research fellowship.

[1] G. J. Long, W. T. Robinson, W. P. Tappmeyer, D. L. Bridges, *J. Chem. Soc., Dalton Trans.* **1973**, 573.
[2] D. N. Hendrickson, S. M. Oh, T.-Y. Doug, T. Kambara, M. J. Cohn, M. F. Moore, *Comments Inorg. Chem.* **1985**, *4*, 329.
[3] J. B. Vincent, H.-R Chang, K. Folting, J. C. Huffman, G. Christou, D. N. Hendrickson, *J. Am. Chem. Soc.* **1987**, *109*, 5703.
[4] R. D. Cannon, U. A. Jayasooriya, R. Wu, S. K. Arapkoske, J. A. Stride, O. F. Nielsen, R. P. White, G. J. Kearly, D. Summerfield, *J. Am. Chem. Soc.* **1994**, *116*, 11869.
[5] R. D. Cannon, R. P. White, *Prog. Inorg. Chem.* **1988**, *36*, 195.
[6] R. Wu, M. Poyraz, F. E. Sowrey, C. E. Anson, S. Wocadlo, A. K. Powell, U. A. Jayasooriya, R. D. Cannon, T. Nakamoto, M. Katada, H. Sano, *Inorg. Chem.* **1998**, *37*, 1913.
[7] T. Fujihara, J. Aonahata, S. Kumakura, A. Nagasawa, K. Murakami, T. Ito, *Inorg. Chem.* **1998**, *37*, 3779.
[8] R. D. Cannon, U. A. Jayasooriya, F. E. Sowrey, C. Tilford, A. Little, J. P. Bourke, R. D. Rogers, J. B. Vincent, G. J. Kearley, *Inorg. Chem.* **1998**, *37*, 5675.
[9] A. M. Bond, R. J. H. Clark, D. G. Humphrey, P. Panayiotopoulos, B. W. Skelton, A. H. White, *J. Chem. Soc., Dalton Trans.* **1998**, 1845.
[10] C. P. Raptopoulou, V. Tangoulis, V. Psycharis, *Inorg. Chem.* **2000**, *39*, 4452.
[11] S. Supriya, S. K. Das, *New J. Chem.* **2003**, *27*, 1568.
[12] E. Bill, C. Krebs, M. Winter, M. Gerdan, A. X. Trautwein, U. Flörke, H.-J. Haupt, P. Chaudhuri, *Chem. Eur. J.* **1997**, *3*, 193.
[13] P. Chaudhuri, M. Hess, T. Weyhermüller, E. Bill, H.-J. Haupt, U. Flörke, *Inorg. Chem. Commun.* **1998**, *1*, 39.
[14] S. G. Sreerama, S. Pal, *Inorg. Chem.* **2002**, *41*, 4843.
[15] W. J. Geary, *Coord. Chem. Rev.* **1971**, *7*, 81.
[16] J. G. Mohanty, R. P. Singh, A. Chakravorty, *Inorg. Chem.* **1975**, *14*, 2178.
[17] F. Birkelbach, T. Weyhermüller, M. Lengen, M. Gerdan, A. X. Trautwein, K. Weighardt, P. Chaudhuri, *J. Chem. Soc., Dalton Trans.* **1997**, 4529.
[18] S. N. Pal, S. Pal, *J. Chem. Soc., Dalton Trans.* **2002**, 2102.
[19] G. R. Desiraju, *Angew. Chem. Int. Ed. Engl.* **1995**, *34*, 2328.
[20] M. G. Davidson, A. E. Goeta, J. A. K. Howard, S. Lamb, S. A. Mason, *New J. Chem.* **2000**, *24*, 477.
[21] S. N. Pal, K. R. Radhika, S. Pal, *Z. Anorg. Allg. Chem.* **2001**, *627*, 1631.
[22] S. N. Pal, S. Pal, *Eur. J. Inorg. Chem.* **2003**, 4244.
[23] K. Kambe, *J. Phys. Soc. Jpn.* **1950**, *5*, 48.
[24] G. V. R. Chandramouli, C. Balagopalakrishna, M. V. Rajasekharan, P. T. Manoharan, *Comput. Chem.* **1996**, *20*, 353.
[25] V. E. Uhlig, M. Friedrich, *Z. Anorg. Allg. Chem.* **1966**, *343*, 299.
[26] W. E. Hatfield, *Theory and Applications of Molecular Paramagnetism* (Eds.: E. A. Boudreaux, L. N. Mulay), Wiley, New York, **1976**, p. 491.
[27] A. C. T. North, D. C. Philips, F. S. Mathews, *Acta Crystallogr., Sect. A* **1968**, *24*, 351.
[28] L. J. Farrugia, *J. Appl. Crystallogr.* **1999**, *32*, 837.
[29] G. M. Sheldrick, *SHELX-97, Structure Determination Software*, University of Göttingen, Göttingen, Germany, **1997**.
[30] P. McArdle, *J. Appl. Crystallogr.* **1995**, *28*, 65.
[31] A. L. Spek, *PLATON, A Multipurpose Crystallographic Tool*, Utrecht University, Utrecht, The Netherlands, **2002**.

Received May 22, 2004
Early View Article
Published Online October 18, 2004

